

Direct evaluation of the temperature dependence of the rate constant based on the quantum instanton approximation

Marcin Buchowiecki^{1,2} and Jiří Vaníček^{1,*}

¹Laboratory of Theoretical Physical Chemistry, Institut des Sciences et Ingénierie Chimiques, École Polytechnique Fédérale de Lausanne (EPFL), CH-1015 Lausanne, Switzerland

²Institute of Physics, University of Szczecin, Wielkopolska 15, 70-451 Szczecin, Poland

(Dated: May 21, 2018)

A general method for the direct evaluation of the temperature dependence of the quantum-mechanical reaction rate constant in many-dimensional systems is described. The method is based on the quantum instanton approximation for the rate constant, thermodynamic integration with respect to the inverse temperature, and the path integral Monte Carlo evaluation. It can describe deviations from the Arrhenius law due to the coupling of rotations and vibrations, zero-point energy, tunneling, corner-cutting, and other nuclear quantum effects. The method is tested on the Eckart barrier and the full-dimensional $\text{H} + \text{H}_2 \rightarrow \text{H}_2 + \text{H}$ reaction. In the temperature range from 300 K to 1500 K, the error of the present method remains within 13% despite the very large deviations from the Arrhenius law. The direct approach makes the calculations much more efficient, and the efficiency is increased even further (by up to two orders of magnitude in the studied reactions) by using optimal estimators for reactant and transition state thermal energies. Which of the estimators is optimal, however, depends on the system and the strength of constraint in a constrained simulation.

I. INTRODUCTION

The measurement of the temperature dependence of the rate constant is one of the important tools of chemical kinetics in determining mechanisms of chemical reactions.^{1–3} Significant deviations from a simple exponential behavior can be evidence of tunneling and of other nuclear quantum effects.^{4,5} These effects are particularly strong for hydrogen transfer reactions with a high activation barrier or at low temperatures. Recently, however, quantum effects have been observed also in many enzymatic reactions at physiological temperatures.^{6–9} It therefore becomes more and more important to have accurate theoretical methods for computing the temperature dependence of the rate constant.¹⁰

Probably the oldest yet still the best known expression for the thermal rate constant $k(T)$ at temperature T is the empirical Arrhenius law,¹¹

$$k_A(T) = Ae^{-E_a/k_B T}. \quad (1.1)$$

Here k_B is the Boltzmann constant, E_a the activation energy, and the temperature dependence is purely exponential. An improvement over the Arrhenius law was provided by the transition state theory (TST),^{12–14} in which

$$k_{\text{TST}}(T) = \frac{k_B T}{h} \frac{Q^\ddagger(T)}{Q_r(T)} e^{-\Delta E^\ddagger/k_B T}, \quad (1.2)$$

where h is the Planck's constant, $Q^\ddagger(T)$ and $Q_r(T)$ are the partition functions of the transition state and the reactants, respectively, and ΔE^\ddagger is the barrier height for the reaction. Here the temperature dependence includes a fractional power T^α in addition to the exponential. Nevertheless, both Arrhenius law and TST are basically purely classical, so they cannot take into account tunneling and other nuclear quantum effects.

Although the simplest quantum effects *can* be taken into account within the TST in an *ad hoc* fashion, by replacing the partition functions by their quantum analogs for the simple harmonic oscillator (which takes into account the zero-point energy, the Wigner tunneling correction,¹⁵ and approximate quantization of the vibrational motion), a more systematic approach requires quantum treatment of the nuclear motion. This is of course extremely difficult, and therefore various approximate yet accurate methods have been developed. These include, e.g., the semiclassical methods^{16–19} or the so-called quantum transition state theories.^{20–28}

In this paper, we evaluate the temperature dependence of the rate constant starting from the quantum instanton (QI) approximation.²⁸ This quantum transition state theory has been shown to describe correctly not only all of the above-mentioned quantum effects, but also corner-cutting, coupling of vibrational and rotational motions, multiple tunneling paths, etc. As we evaluate the temperature dependence of the rate constant directly, we can speed up the QI calculation significantly by avoiding the tedious umbrella sampling necessary for computing the rate constant itself. Furthermore, if it is only the temperature dependence of the rate constant that is needed, we can increase the accuracy of the QI approximation for the rate constant by canceling some small remaining systematic errors. This can be useful, e.g., if we know $k(T_0)$ at a temperature T_0 very accurately and would like to know $k(T)$ at other temperatures. The temperature dependence of the rate constant is computed via a thermodynamic integration^{29,30} with respect to the inverse temperature. A similar thermodynamic integration in the framework of the QI model was used by Ceotto and Miller to compute the rate constant for several one and two-dimensional systems using a discrete variable representation.³¹ Below, we develop a general thermodynamic integration procedure based on the path integral

implementation, which is suitable for many-dimensional systems.

The method is tested on two simple systems for which exact quantum dynamical calculations are feasible: the Eckart barrier and the full nine-dimensional $\text{H} + \text{H}_2 \rightarrow \text{H}_2 + \text{H}$ reaction. While the former system is the simplest one-dimensional model of a bimolecular reaction, the latter is the simplest bimolecular chemical reaction with an energy barrier. As such, it has been widely studied and attained the status of a benchmark reaction.^{32,33} Despite the apparent simplicity, this reaction remains a challenging test for new approximations. This is due to the presence of strong quantum effects, as the lightest atoms are involved in both bond breaking and bond formation. This reaction was investigated not only for the temperature dependence of its rate constant, but also for the kinetic isotope effect,^{34–36} the presence of the geometric phase effect,^{37,38} etc.

The remainder of this paper is organized as follows: Section II describes the methodology, i.e., the QI approximation, the thermodynamic integration with respect to the inverse temperature, the path integral formalism, and the relevant estimators. Computational details and, in particular, the analysis of various errors are presented in Sec. III. Section IV contains the results. First, it is shown how the low and high temperature limits are obtained. The numerical results for the Eckart barrier and the $\text{H} + \text{H}_2$ reaction are then presented. The results are compared with the Arrhenius law, TST, TST with the Wigner tunneling correction, and the exact quantum calculation. Finally, we discuss how the efficiency is related to the dependence of the statistical error on the number of imaginary time slices in the path integral, and how this error, in turn, depends on the system under study. Section V concludes the paper.

II. METHODOLOGY

A. Quantum instanton approximation for the thermal rate constant

The QI approximation for thermal rate constants was introduced in Ref. 28. The most direct derivation^{35,39,40} starts from the exact Miller-Schwartz-Tromp formula for the rate constant,⁴¹

$$k(T)Q_r = \int_0^\infty dt C_{\text{ff}}(\beta, t) \quad (2.1)$$

where $C_{\text{ff}}(\beta, t)$ is the symmetrized flux-flux correlation function,

$$C_{\text{ff}}(\beta, t) = \text{Tr} \left(e^{-\beta\hat{H}/2} \hat{F}_a e^{-\beta\hat{H}/2} e^{i\hat{H}t/\hbar} \hat{F}_b e^{-i\hat{H}t/\hbar} \right), \quad (2.2)$$

with Hamiltonian operator \hat{H} , inverse temperature $\beta := 1/k_B T$, time t , and \hat{F}_γ the flux operator through the dividing surface γ . A stationary-phase approximation

applied to Eq. (2.1) yields the QI approximation for the rate constant,^{35,40}

$$k(T) \approx k_{\text{QI}}(T) = \frac{1}{Q_r} C_{\text{ff}}(\beta, 0) \frac{\sqrt{\pi}}{2} \frac{\hbar}{\Delta H(\beta)} \quad (2.3)$$

where $\Delta H(\beta)$ is a specific type of energy variance,³⁴

$$\Delta H(\beta) = \hbar \left[\frac{-\ddot{C}_{dd}(\beta, 0)}{2C_{dd}(\beta, 0)} \right]^{1/2}. \quad (2.4)$$

The delta-delta correlation function used above is defined as

$$C_{dd}(\beta, t) = \text{Tr} \left(e^{-\beta\hat{H}/2} \hat{\Delta}_a e^{-\beta\hat{H}/2} e^{i\hat{H}t/\hbar} \hat{\Delta}_b e^{-i\hat{H}t/\hbar} \right) \quad (2.5)$$

where the generalized delta function operator is given by

$$\hat{\Delta}_\gamma = \Delta [\xi(\hat{\mathbf{r}}) - \xi_\gamma] \equiv \delta [\xi(\hat{\mathbf{r}}) - \xi_\gamma] m^{-1/2} \|\nabla \xi\| \quad (2.6)$$

and $\xi(\mathbf{r})$ is the reaction coordinate such that $\xi(\mathbf{r}^\ddagger) = 0$ at the transition state. Similarly, $\xi(\mathbf{r}) = \xi_\gamma$ defines the position of the dividing surface γ . We have used mass-scaled coordinates in which all degrees of freedom have the same mass m . In practice, the exact delta function constraint is approximated by a Gaussian constraint corresponding to a harmonic constraint potential $V_{\text{constr}}(\mathbf{r})$,^{34,35}

$$\delta[\xi(\mathbf{r}) - \xi_\gamma] \approx \sqrt{\frac{\beta}{2\pi\sigma^2}} e^{-\beta V_{\text{constr}}(\mathbf{r})}, \quad (2.7)$$

$$V_{\text{constr}}(\mathbf{r}) = \frac{1}{2} \left(\frac{\xi(\mathbf{r}) - \xi_\gamma}{\sigma} \right)^2. \quad (2.8)$$

The accuracy of the QI approximation has been already verified in numerous applications.^{28,34,35,42–47} The main shortcoming of the QI method is the neglect of recrossing which is however, neglected in any quantum or classical transition state theories. The recrossing effects on the quantum instanton rate constant have been quantified for several collinear reactions by Ceotto and Miller.³¹ Fortunately, the recrossing effects become generally less important in higher dimensions.

B. Temperature dependence via the thermodynamic integration

The goal of this paper is to compute the temperature dependence of the rate constant, i.e., the ratio $k(T_2)/k(T_1)$. Within the QI approximation, this ratio is given by

$$\frac{k(T_2)}{k(T_1)} = \frac{Q_r(\beta_1)}{Q_r(\beta_2)} \frac{\Delta H(\beta_1)}{\Delta H(\beta_2)} \frac{C_{\text{ff}}(\beta_2, 0)}{C_{\text{ff}}(\beta_1, 0)} \frac{C_{\text{dd}}(\beta_2, 0)}{C_{\text{dd}}(\beta_1, 0)}, \quad (2.9)$$

where we multiplied and divided the numerator and denominator by $C_{\text{dd}}(\beta, 0)$. In this expression, quantities

$\Delta H(\beta)$ and $C_{\text{ff}}(\beta, 0)/C_{\text{dd}}(\beta, 0)$ can be computed directly by the Metropolis Monte-Carlo procedure because they are thermodynamic averages. On the other hand, the ratios $Q_r(\beta_1)/Q_r(\beta_2)$ and $C_{\text{dd}}(\beta_2, 0)/C_{\text{dd}}(\beta_1, 0)$ cannot be computed this way since they involve ratios of quantities at different temperatures. These ratios can, however, be calculated by the method of *thermodynamic integration*^{29,30} with respect to the inverse temperature β ,

$$\frac{Q_r(\beta_2)}{Q_r(\beta_1)} = \exp \left[- \int_{\beta_1}^{\beta_2} E_r(\beta) d\beta \right], \quad (2.10)$$

$$\frac{C_{\text{dd}}(\beta_2, 0)}{C_{\text{dd}}(\beta_1, 0)} = \exp \left[- \int_{\beta_1}^{\beta_2} E^\ddagger(\beta) d\beta \right], \quad (2.11)$$

where E_r and E^\ddagger are the thermal energies of the reactants and of the transition state, respectively. A similar thermodynamic integration was used within a discrete variable representation of the QI approximation to compute the rate constant for several collinear triatomic reactions.³¹ Unlike Q_r and C_{dd} , the energies are normalized quantities because they can be written as logarithmic derivatives:

$$E_r(\beta) := - \frac{d \log Q_r(\beta)}{d\beta} = - \frac{dQ_r(\beta)/d\beta}{Q_r(\beta)}, \quad (2.12)$$

$$E^\ddagger(\beta) := - \frac{d \log C_{\text{dd}}(\beta, 0)}{d\beta} = - \frac{dC_{\text{dd}}(\beta, 0)/d\beta}{C_{\text{dd}}(\beta, 0)}. \quad (2.13)$$

Hence they can be computed directly by a Monte Carlo procedure.

C. Path integral representation of relevant quantities

Quantum thermodynamic effects can be treated rigorously using the imaginary time path integral (PI).⁴⁸⁻⁵² Let D be the number of degrees of freedom ($D = 1$ for the Eckart barrier and $D = 9$ for the H_3 potential) and P the number of imaginary time slices in the PI. The PI representations of the partition function⁴⁹⁻⁵² and the delta-delta correlation function³⁴ are

$$Q_r^P(\beta) = C \int d\mathbf{r}^{(1)} \dots \int d\mathbf{r}^{(P)} \exp \left[-\beta \Phi \left(\left\{ \mathbf{r}^{(s)} \right\} \right) \right], \quad (2.14)$$

$$C_{\text{dd}}^P(\beta, 0) = C \int d\mathbf{r}^{(1)} \dots \int d\mathbf{r}^{(P)} \Delta \left[\xi_a \left(\mathbf{r}^{(0)} \right) \right] \times \Delta \left[\xi_b \left(\mathbf{r}^{(P/2)} \right) \right] \exp \left[-\beta \Phi \left(\left\{ \mathbf{r}^{(s)} \right\} \right) \right], \quad (2.15)$$

where $C = [mP/(2\pi\hbar^2\beta)]^{DP/2}$, $\mathbf{r}^{(s)}$ is a D -dimensional vector representing the s th time slice, and the effective

potential Φ is given by

$$\Phi \left(\left\{ \mathbf{r}^{(s)} \right\} \right) = \frac{mP}{2\hbar^2\beta^2} \sum_{s=1}^P \left(\mathbf{r}^{(s)} - \mathbf{r}^{(s-1)} \right)^2 + \frac{1}{P} \sum_{s=1}^P V \left(\mathbf{r}^{(s)} \right). \quad (2.16)$$

For $P = 1$, the above expressions reproduce classical statistical mechanics, while exact quantum statistics is reached in the limit $P \rightarrow \infty$.

In practice, there are two main strategies for evaluating thermodynamic averages using the PI: the PI molecular dynamics (PIMD)^{50,53} or PI Monte Carlo (PIMC).⁵² We use the PIMC procedure together with the Metropolis algorithm. The basic idea is to sample the PI configuration space according to an appropriate weight ρ , which is, e.g., for C_{dd} given by

$$\rho^\ddagger \left(\left\{ \mathbf{r}^{(s)} \right\} \right) := \Delta \left[\xi_a \left(\mathbf{r}^{(0)} \right) \right] \Delta \left[\xi_b \left(\mathbf{r}^{(P/2)} \right) \right] \exp \left[-\beta \Phi \left(\left\{ \mathbf{r}^{(s)} \right\} \right) \right], \quad (2.17)$$

and then, at each sampled configuration, to evaluate the so-called estimator $A^P(\{\mathbf{r}^{(s)}\})$ of the relevant physical quantity A . The final estimate of A is given by the average $\langle A^P \rangle$ along the PIMC trajectory.

Using the PI representation of Q_r and C_{dd} , one can obtain estimators for all quantities needed in Eq. (2.9), i.e., ΔH , $C_{\text{ff}}/C_{\text{dd}}$, and the logarithmic derivatives of Q_r , C_{dd} (i.e., the energies E_r , E^\ddagger). Those for ΔH and $C_{\text{ff}}/C_{\text{dd}}$ are listed in Ref. 34.

D. Estimators for E_r

The simplest estimator for the energy E_r , the so-called Barker or thermodynamic estimator (TE),⁵⁴ can be derived directly from Eq. (2.12) and the PI expression (2.14), giving

$$E_{r,\text{TE}}^P = \frac{DP}{2\beta} - \frac{mP}{2\beta^2} \sum_{s=1}^P \left(\mathbf{r}^{(s)} - \mathbf{r}^{(s-1)} \right)^2 + \frac{1}{P} \sum_{s=1}^P V \left(\mathbf{r}^{(s)} \right). \quad (2.18)$$

As observed by Herman *et al.*,⁵⁵ the TE can have a large statistical error, which can be avoided with the so-called virial (VE)⁵⁵ or centroid virial (CVE),⁵⁶ estimators. Invoking the virial theorem, the kinetic energy in these two estimators is replaced by an expression involving the gradient of the potential energy.⁵⁵ This is convenient in the PIMD implementations since the gradient is already available. In PIMC simulations, however, only the potential is needed for the random walk, and in order to avoid computing the gradients, alternative approaches have been proposed. One can, e.g., employ the centroid thermodynamic estimator⁵⁷ or more generally, use a procedure based on rescaling coordinates^{58,59} in which the gradients of the potential are replaced by a single derivative that can be evaluated by finite difference.⁶⁰ Variants of the latter approach have been applied successfully to compute thermal energies and heat capacities,⁶⁰ kinetic isotope effects^{45,61}, equilibrium isotope effects⁶², or the

derivatives of the flux-flux correlation function⁶³ needed in the generalized QI model.³⁹

The VE for E_r can be derived most directly by the change of coordinates $\mathbf{x}^{(s)} := \beta^{-1/2}\mathbf{r}^{(s)}$ in the PI (2.14), yielding

$$\begin{aligned} E_{r,\text{VE}}^P &= \frac{1}{P} \sum_{s=1}^P \left\{ V(\mathbf{r}^{(s)}) + \beta \frac{dV[(\beta + \Delta\beta)^{1/2}\beta^{-1/2}\mathbf{r}^{(s)}]}{d\Delta\beta} \right\} \\ &= \frac{1}{P} \sum_{s=1}^P \left\{ V(\mathbf{r}^{(s)}) + \frac{dV[(1+q)^{1/2}\mathbf{r}^{(s)}]}{dq} \right\}, \end{aligned} \quad (2.19)$$

where q is a small dimensionless parameter and the q -derivative is evaluated by finite difference at $q = 0$. Similarly, the CVE can be obtained by the change of variables $\mathbf{x}^{(s)} := \beta^{-1/2}(\mathbf{r}^{(s)} - \mathbf{r}^{(C)})$, where one first subtracts the so-called centroid coordinate $\mathbf{r}^{(C)} := P^{-1} \sum_{s=1}^P \mathbf{r}^{(s)}$. The resulting estimator is

$$\begin{aligned} E_{r,\text{CVE}}^P &= \frac{D}{2\beta} + \\ &+ \frac{1}{P} \sum_{s=1}^P \left\{ V(\mathbf{r}^{(s)}) + \frac{dV[\mathbf{r}^{(C)} + (1+q)^{1/2}(\mathbf{r}^{(s)} - \mathbf{r}^{(C)})]}{dq} \right\}. \end{aligned} \quad (2.20)$$

E. Estimators for E^\ddagger

In the case of constrained simulations near the transition state, the constrained weight function (2.17) can be approximated by using the Gaussian approximation of the delta function from Eqs. (2.7)-(2.8). Besides a prefactor, this amounts to adding a constraint potential

$$\Phi_{\text{constr}}(\{\mathbf{r}^{(s)}\}) := V_{\text{constr}}(\mathbf{r}^{(P/2)}) + V_{\text{constr}}(\mathbf{r}^{(P)})$$

to the effective potential Φ . Assuming that V_{constr} is independent of temperature and following a derivation similar to that for estimators of E_r , one obtains the thermodynamic, virial, and centroid virial estimators for E^\ddagger ,

$$E_{\text{TE}}^{\ddagger,P} = E_{r,\text{TE}}^P - \frac{1}{\beta} + \Phi_{\text{constr}}(\{\mathbf{r}^{(s)}\}), \quad (2.21)$$

$$\begin{aligned} E_{\text{VE}}^{\ddagger,P} &= E_{r,\text{VE}}^P - \frac{1}{\beta} + \Phi_{\text{constr}}(\{\mathbf{r}^{(s)}\}) \\ &+ \frac{d\Phi_{\text{constr}}[(1+q)^{1/2}\{\mathbf{r}^{(s)}\}]}{dq}, \end{aligned} \quad (2.22)$$

$$\begin{aligned} E_{\text{CVE}}^{\ddagger,P} &= E_{r,\text{CVE}}^P - \frac{1}{\beta} + \Phi_{\text{constr}}(\{\mathbf{r}^{(s)}\}) \\ &+ \frac{d\Phi_{\text{constr}}[\{\mathbf{r}^{(C)} + (1+q)^{1/2}(\mathbf{r}^{(s)} - \mathbf{r}^{(C)})\}]}{dq}. \end{aligned} \quad (2.23)$$

Although the above estimators converge to the exact results, we found that the statistical errors can be decreased slightly by employing an alternative set of estimators, derived using an exact relation

$$\langle \Phi_{\text{constr}}(\{\mathbf{r}^{(s)}\}) \rangle = \beta^{-1},$$

which is valid for a harmonic constraint potential for any value of P . The new estimators are

$$E_{\text{TE}}^{\ddagger,P} = E_{r,\text{TE}}^P, \quad (2.24)$$

$$E_{\text{VE}}^{\ddagger,P} = E_{r,\text{VE}}^P + \frac{d\Phi_{\text{constr}}[(1+q)^{1/2}\{\mathbf{r}^{(s)}\}]}{dq}, \quad (2.25)$$

$$E_{\text{CVE}}^{\ddagger,P} = E_{r,\text{CVE}}^P + \frac{d\Phi_{\text{constr}}[\{\mathbf{r}^{(C)} + (1+q)^{1/2}(\mathbf{r}^{(s)} - \mathbf{r}^{(C)})\}]}{dq}. \quad (2.26)$$

Estimators (2.24)-(2.26) are in a way more intuitive than estimators (2.21)-(2.23): in the limit of a sharp constraint, the constrained energy should be independent of the type of constraint.

It should be stressed that the last terms in the VE and CVE in Eqs. (2.22), (2.23), (2.25), and (2.26) are important; without them the agreement among the TE, VE, and CVE is lost. In other words, an intuitive guess such as $E_{\text{CVE}}^{\ddagger,P} = E_{r,\text{CVE}}^P$ would not give a correct answer for the constrained energy.

Finally, we also tested a constraint potential that is proportional to temperature, i.e.,

$$V_{\text{constr}} = \beta^{-1} \tilde{V}_{\text{constr}}, \quad (2.27)$$

where $\tilde{V}_{\text{constr}}$ is a harmonic potential independent of temperature. As a result, the constraint (2.7) itself is actually independent of temperature. Following again a derivation similar to that for estimators of E_r , one obtains another set of the TE, VE, and CVE for E^\ddagger , that look exactly like the estimators (2.24)-(2.26) for V_{constr} independent of temperature. The only difference is that the random walk is done with a different constraint.

III. COMPUTATIONAL DETAILS AND ERROR ANALYSIS

All calculations were performed with a PIMC code implemented in Fortran 90. Sampling of the configurational space in the PIMC simulation was done using three types of moves. Staging algorithm⁶⁴ was employed to move all unconstrained beads. Constrained beads, i.e., beads $s = P/2$ and $s = P$ which feel the constraint potential V_{constr} , were sampled with the free particle single slice algorithm.⁵² Finally, whole chain moves⁵² were used to speed up sampling of the potential energy surface.

The Gaussian constraint potential must be strong enough in order to exert the constraining effect on the system. When this condition was satisfied, the converged results were independent of the constraint. However, the statistical root mean square error (RMSE) of the transition state energy E^\ddagger increases with the strength of the constraint because sampling of the configuration space becomes more difficult. Therefore the selected strength of the constraint should take into account these two effects. We have used $k = 10$ a.u. in both systems.

All quantities needed in the ratio (2.9) were evaluated using the above mentioned estimators. The thermodynamic integrations (2.10) and (2.11) were evaluated with the Simpson rule using 25 values of β between $\beta_0 = 1/k_B T_0$ and $\beta_{\max} = 1/k_B T_{\min}$ with the reference temperature $T_0 = 1500$ K and the minimum temperature $T_{\min} = 200$ K. The number of beads was chosen to be inversely proportional to the temperature, with the maximal number of beads (used for $T_{\min} = 200$ K) being $P = 96$ for the Eckart barrier and $P = 160$ for the $\text{H} + \text{H}_2$ reaction.

The error of the final result consists of four main error contributions: a) the statistical error due to the Monte Carlo simulation, b) the error due to the discretization of the TI, c) the error due to the discretization of the PI (i.e., the “finite P error”), and d) the actual error of the QI approximation. We have carefully separated these four contributions and attempted to make the first three contributions small in comparison with the error of the QI. In more complicated systems, this may not be possible and especially the final statistical error may be comparable to or larger than the error of the QI. Because the exponentiation of the TI is quite sensitive to various errors, a detailed analysis of errors was carried out for the ratio $k(200 \text{ K})/k(1500 \text{ K})$, i.e., over the largest temperature range, where the first three types of errors are the greatest. The TI was evaluated by four different numerical methods, namely the trapezoidal, Simpson, Simpson 3/8, and Boole methods.⁶⁵

Comparing the analytical bounds on the *discretization errors* of the TI integrals using a numerical estimate of a higher order derivative,⁶⁵ one can conclude that both the Simpson and Simpson 3/8 methods were much better than the trapezoidal rule and that the Boole method did not provide any further improvement. Specifically, for the Eckart barrier the error of the ratio due to the discretization of the TI was 2%, 0.03%, 0.02%, or 0.04% for the trapezoidal, Simpson, Simpson 3/8, or Boole methods, respectively. For the $\text{H} + \text{H}_2$ reaction, the discretization error of the final ratio was 7%, 0.3%, 0.1%, or 0.3%, in the same order. It should be emphasized that these error estimates are very conservative, as the actual difference between the final ratios based on different methods was an order of magnitude smaller than what one would expect from the error estimates. The final results displayed in the plots used the Simpson method.

The *statistical* RMSEs were estimated with the block averaging method using a variable block size⁶⁶ to remove correlation of the PIMC data. The statistical error of the TI was evaluated using an appropriate formula for each integration method and assuming that the statistical errors of energies at different temperatures were uncorrelated. As expected, the statistical error did not depend much on the integration method, and was always close to the statistical error for the Simpson method. The statistical error of the final ratio was 0.3% for the Eckart barrier and 1.6% for the $\text{H} + \text{H}_2$ reaction.

The *finite P error*, i.e., the error due to the discretiza-

tion of the Feynman PI, was obtained by repeating calculations of all quantities at all temperatures with twice smaller numbers of beads ($P \rightarrow P/2$) and then extrapolating each quantity to $P \rightarrow \infty$, assuming $1/P^2$ convergence. We emphasize that we used the extrapolated results only for estimating the finite P error of the computed ratio and *not* for estimating the ratio itself, which could be dangerous. The finite P error of the ratio was -0.3% for the Eckart barrier and -3.5% for the $\text{H} + \text{H}_2$ reaction.

[We note that for $\text{H} + \text{H}_2$ one of the temperatures (972.93 K, a temperature in the vicinity of which a sharp bend in the $E^\ddagger - E_r$ dependence occurs) required a five times longer simulation to reduce the TI discretization errors. This was because a small statistical error had a huge effect on the estimate of the fourth derivative and hence on the analytical estimate of the discretization error.]

To sum up, in both systems the TI discretization error was negligible to the statistical and finite P errors, which, in turn, were small in comparison to the error of the QI approximation.

IV. RESULTS

A. Temperature dependence according to the Arrhenius law, TST, and the TST with the Wigner tunneling correction

At high temperatures, the rate constant is expected to behave classically and follow the Arrhenius law or the more accurate TST result. Whereas the Arrhenius law (1.1) predicts the rate constant ratio to be a simple exponential function of the inverse temperature,

$$\frac{k_A(\beta_2)}{k_A(\beta_1)} = e^{-E_a(\beta_2 - \beta_1)}, \quad (4.1)$$

TST (1.2) gives the ratio of rate constants

$$\frac{k_{\text{TST}}(\beta_2)}{k_{\text{TST}}(\beta_1)} = \frac{\beta_1 Q^\ddagger(\beta_2) Q_r(\beta_1)}{\beta_2 Q^\ddagger(\beta_1) Q_r(\beta_2)} e^{-(\beta_2 - \beta_1)\Delta E^\ddagger}. \quad (4.2)$$

In particular, assuming the partition functions Q^\ddagger and Q_r to be separable into products of classical rotational and vibrational partition functions, the temperature dependence (4.2) of TST rate constant includes an additional fractional power law besides the exponential dependence in the Arrhenius law (4.1).

At somewhat lower temperatures, when quantum effects start to play a role, the basic TST expression (4.2) can be improved in several ways: First, classical partition functions Q_r and Q^\ddagger can be replaced by their exact quantum analogs for a harmonic potential. Second, quantum tunneling can be included approximately via the Wigner tunneling correction.¹⁵ This method corrects

the rate constant with a multiplicative factor

$$\kappa = 1 + \frac{h^2 |\nu^\ddagger|^2 \beta^2}{24}, \quad (4.3)$$

where ν^\ddagger is the imaginary frequency of the asymmetric stretch along the reaction coordinate. The correction can be derived by treating the motion through the transition state as a vibration on an upside down potential and expanding the quantum partition function to second order in β . Although an improvement over TST, the Wigner tunneling correction cannot describe multi-dimensional tunneling.

B. Eckart barrier

A simple model of an activated chemical reaction is provided by the Eckart barrier, a one-dimensional system described by the potential

$$V(x) = V_0 [\cosh(ax)]^{-2}. \quad (4.4)$$

We use standard parameter values $V_0 = 1.56 \cdot 10^{-2}$ a.u., $a = 1.36$ a.u., mass $m = 1060$ a.u. and reaction coordinate $\xi := x$. The exact quantum rate constant k_{QM} for this reaction can be obtained by integrating the exact quantum mechanical cumulative reaction probability, which is known analytically.⁶⁷

Figure 1 (a) compares the QI results with the exact QM results, TST (which is equal to the Arrhenius law here), and the TST including the Wigner tunneling correction. The reference temperature is 1500 K and the plot shows ratios for temperatures down to 200 K. Since classical recrossing does not occur for the Eckart barrier, all TSTs should converge to the correct quantum results at high temperatures. The figure confirms that this is indeed the case: note that all curves are tangent at the high temperature limit. At low temperatures, one reaches the quantum regime where tunneling is important and consequently the Arrhenius plot of the exact QM result has a large curvature. While TST has a huge error, the QI approximation agrees very well with the QM result. Note that the Wigner tunneling correction improves over the TST and captures the tunneling effect partially but still fails to recover the curvature of the exact result.

Figure 1 (b) shows the relative error of the rate constant ratio for the different methods. Whereas both TST and TST with the Wigner tunneling correction deteriorate rapidly with decreasing temperature, the QI method has an error below 3% for all temperatures above 330 K. The QI approximation has a significant error ($\geq 10\%$) only at very low temperatures, below ~ 270 K. However, this error was well understood already in the original paper by Miller et al.²⁸ and can be remedied by considering two separate dividing surfaces at very low temperatures. (Here we have used a single dividing surface at all temperatures for simplicity.)

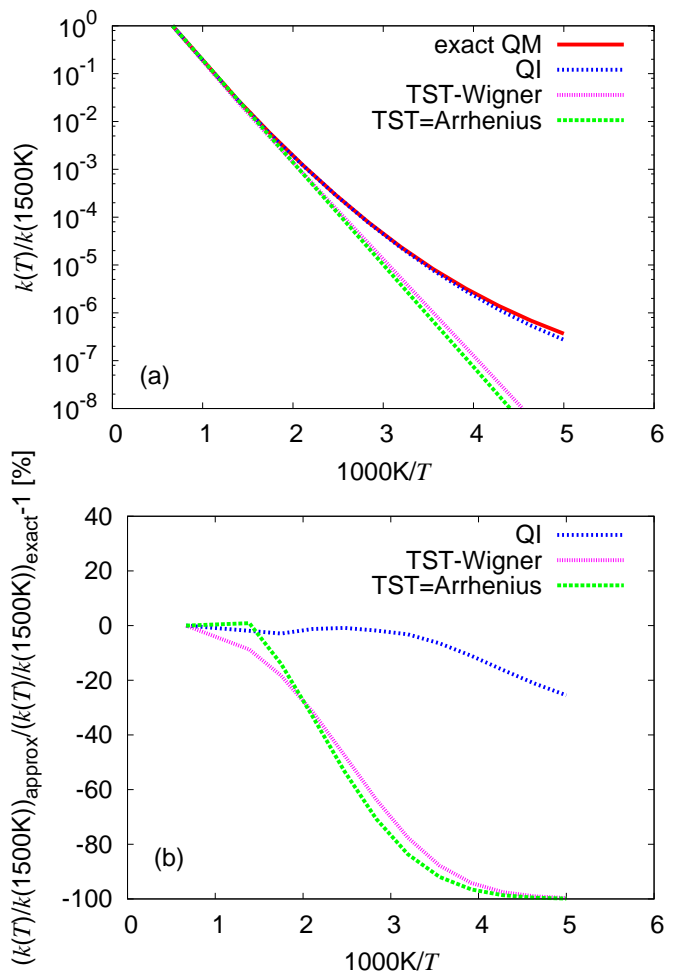


FIG. 1: Eckart barrier. (a) Temperature dependence of the rate constant. (b) Temperature dependence of the relative error of the ratio $k(T)/k(1500\text{K})$.

The temperature dependence of the reactant and transition state energies is shown in Fig. 2. While both curves are quite smooth, small discretization errors in the integrals can have large effects on the exponentiated result. By a detailed error analysis described in Sec. III, we found that the Simpson method was sufficient for the TI over the whole temperature range. Note that the VE for E_r gives zero, but can be easily corrected with an analytical correction $1/(2\beta)$.

The three different estimators for the constrained energy E^\ddagger at $T = 515.15$ K are compared in Figs. 3 and 4. Panel (a) of Fig. 3, which uses the simpler estimators (2.24)-(2.26), shows that the TE, VE, and CVE agree for all examined values of P and, in particular, converge to the same value for $P \rightarrow \infty$. The three estimators, however, differ in their statistical convergence. Unlike for the unconstrained result, where the CVE is the optimal estimator, for the constrained energy, the optimal estimator is the VE. This can be clearly seen in Fig. 3 (b) which shows the RMSEs of the different estimators for different values of P . While the RMSE of the TE increases

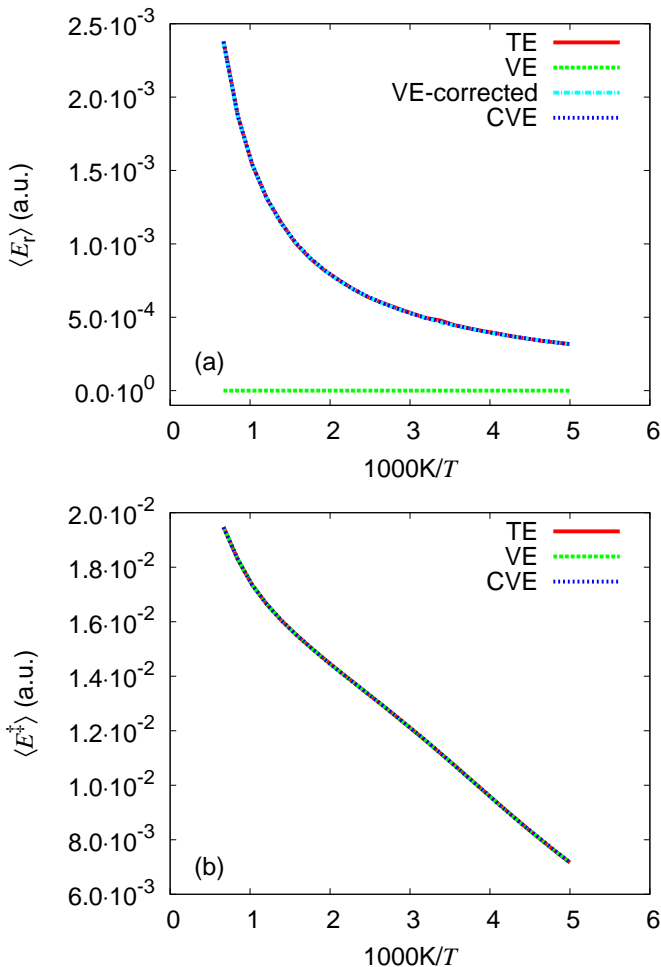


FIG. 2: Eckart barrier. Temperature dependence of the reactant (a) and transition state (b) energies.

with P , the RMSEs of the VE and CVE remain approximately constant as a function of P , with the VE having a much smaller statistical error. Assuming that the desired convergence is achieved for $P = 24$, the speedup factor achieved by using the VE compared to the TE and CVE is approximately $2.9^2 \approx 8$ and $8.1^2 \approx 60$, respectively. It is clear from the figure that both the speedup factor and the best estimator depend on P and hence on the temperature.

Figure 4 shows the same results, but computed with the estimators (2.21)-(2.23). The statistical errors are very similar, although for the VE slightly larger than those in Fig. 3.

C. The $\text{H} + \text{H}_2 \rightarrow \text{H}_2 + \text{H}$ reaction

The temperature dependence of the rate constant of the $\text{H} + \text{H}_2 \rightarrow \text{H}_2 + \text{H}$ reaction was studied on the Boothroyd-Keogh-Martin-Peterson (BKMP2) reactive potential energy surface.⁶⁸⁻⁷⁰ The classical transition state of this system has a collinear configuration with

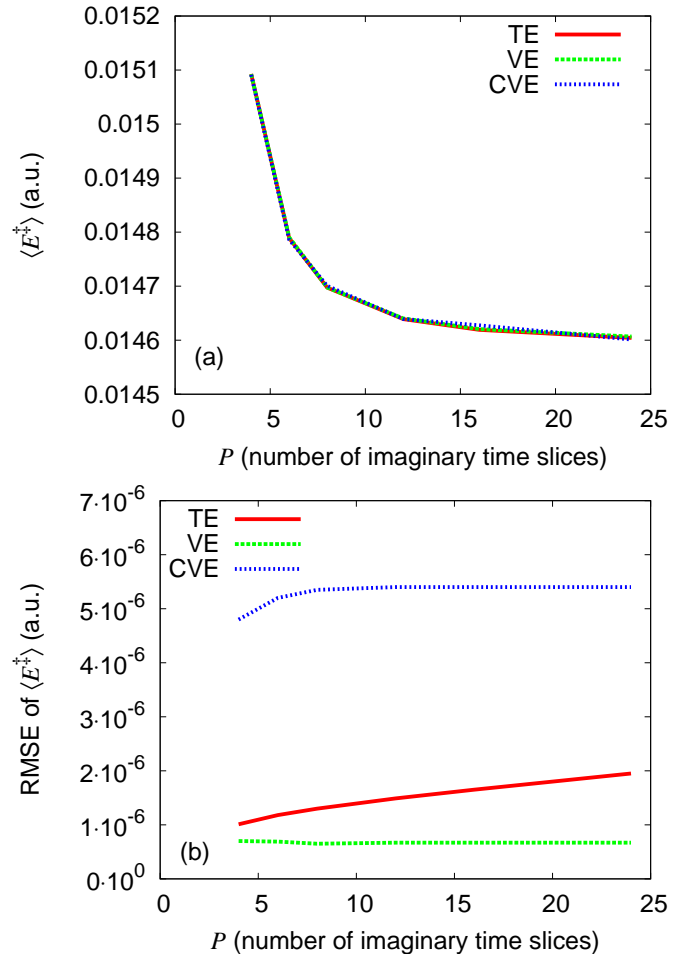


FIG. 3: Dependence of the transition state energy (a) and of the statistical RMSE of the transition state energy (b) on the number of imaginary time slices for the Eckart barrier at $T = 515.15$ K. The constraint potential is independent of temperature and estimators (2.24)-(2.26) are used.

equal bond lengths $d_{\text{H}_a\text{H}_b} = d_{\text{H}_b\text{H}_c}$. A suitable reaction coordinate is therefore given by the difference of the bond lengths,

$$\xi(\mathbf{r}) := d_{\text{H}_a\text{H}_b} - d_{\text{H}_b\text{H}_c}. \quad (4.5)$$

Figure 5 (a) shows the temperature dependence of the rate constant in the range from 200 K to 1500 K. The exact QM results are from Ref. 35. At high temperatures the TST curve is tangent to the exact QM curve, but at low temperatures, there is a significant discrepancy even for the TST with the Wigner tunneling correction. On the other hand, the QI approximation agrees very well with the exact QM result all the way to 200 K. The relative error of the rate constant ratio is shown in Fig. 5 (b) which confirms that the error of the QI approach is within 13% in the full temperature range whereas all other approximations have huge errors already for temperatures as high as 500 K.

In case of the $\text{H} + \text{H}_2 \rightarrow \text{H}_2 + \text{H}$ reaction, the VE had

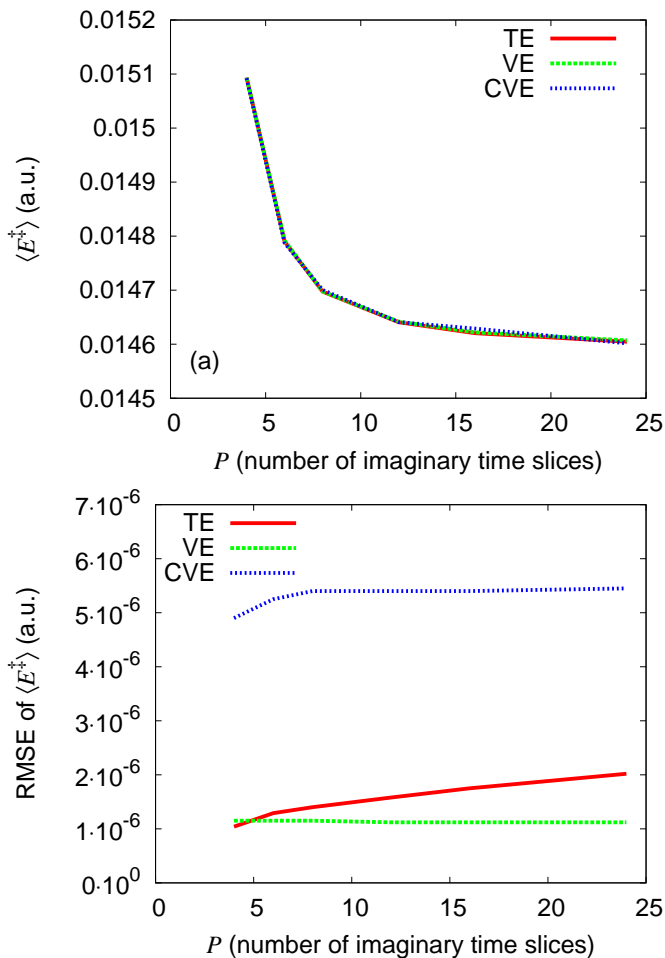
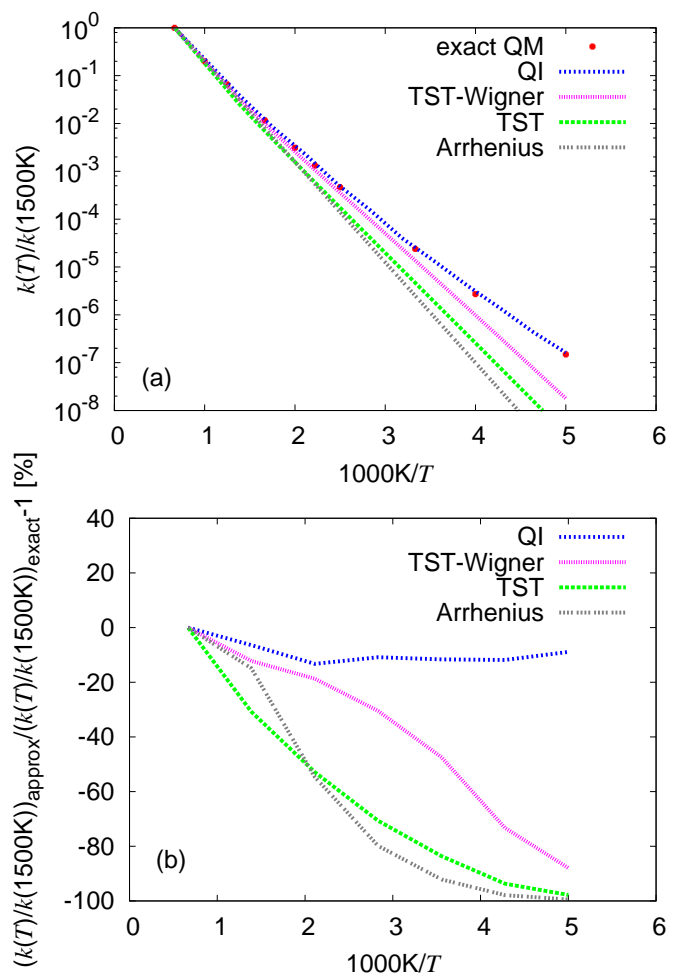


FIG. 4: M. Buchowiecki and J. Vaníček

to be corrected for both E_r and E^\ddagger calculations. The reason is that the virial theorem only holds for bound systems. The transition state of the H_3 system can translate freely as a whole and the three translational degrees of freedom yield a correction of $D/(2\beta) = 3/(2\beta)$ to the VE. In the reactant region, both the H atom and H_2 molecule can move freely and the six translational degrees of freedom give a correction of $6/(2\beta)$ to the VE.

The temperature dependence of the reactant and transition state energies is shown in Fig. 6. While both curves are quite smooth, small discretization errors in the integrals can have large effects on the exponentiated result. By an error analysis described in Sec. III, we found that the Simpson method was sufficient for the TI over the whole temperature range.

Figures 7 and 8 show how the constraint energy E^\ddagger and the RMSE of E^\ddagger depend on P for $T = 515.15$ K. Panel (a) of Fig. 7, which uses the estimators (2.24)-(2.26) and a constraint potential independent of temperature, shows again that the TE, corrected VE, and CVE give approximately the same results for all values of P and, within a statistical error, converge to the same limiting value for $P \rightarrow \infty$. Panel (b) of Fig. 7 shows that while

FIG. 5: The $H + H_2 \rightarrow H_2 + H$ reaction. (a) Temperature dependence of the rate constant. (b) Temperature dependence of the relative error of the ratio $k(T)/k(1500K)$.

the statistical error of the CVE is approximately constant as a function of P , the RMSEs of the TE and VE grow with P . However, in this case, the results are quite well converged for $P = 32$ and at this point the RMSE of the CVE is still larger than the RMSE of the TE, although it is already smaller than the RMSE of the VE. While for lower temperatures where larger values of P are needed, CVE would eventually become the optimal estimator, it is not so for $T = 515.15$ K. The growth of the RMSE of the VE with P is due to the fact that unlike for the Eckart barrier, the transition state of the H_3 system can move freely as a whole.

Finally, Fig. 8 shows analogous results, still using estimators (2.24)-(2.26), but obtained with a constraint potential (2.27) proportional to T (chosen such that the two types of constraints coincide for $T = 515.15$ K). As expected, the statistical errors of the TE, VE, and CVE are similar to those in Fig. 7 [obtained with the constraint potential (2.8) independent of T].

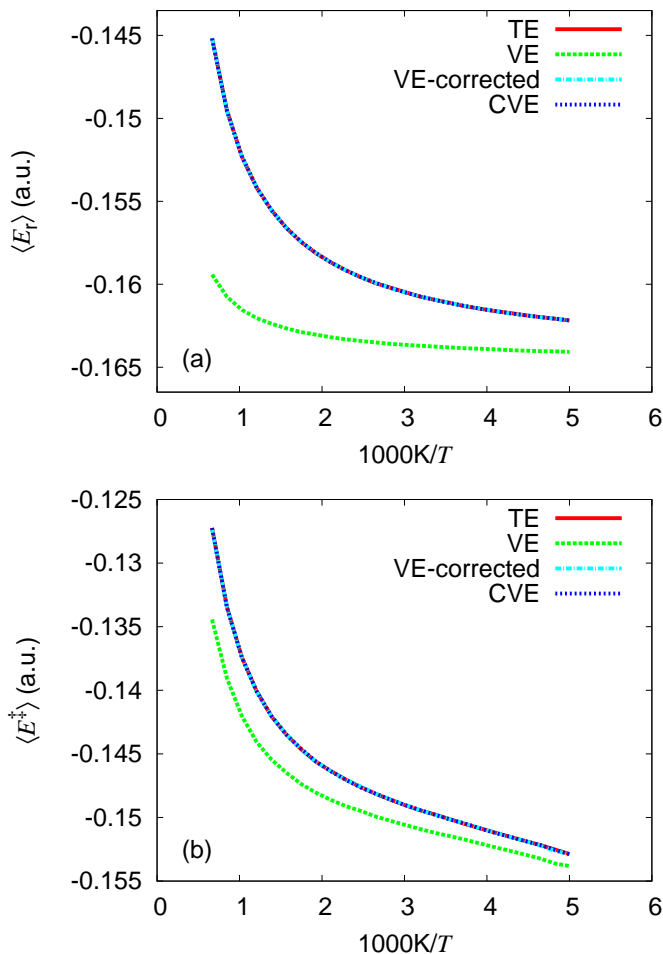


FIG. 6: The $\text{H} + \text{H}_2 \rightarrow \text{H}_2 + \text{H}$ reaction. Temperature dependence of the reactant (a) and transition state (b) energies.

V. CONCLUSIONS

A general method for the direct evaluation of the temperature dependence of the quantum rate constant was presented. The main advantage of this method is the increased efficiency: Evaluating the temperature dependence directly, without computing the rate constant at any given temperature, allows us to avoid a tedious umbrella sampling procedure.

Besides efficiency, the direct calculation of the temperature dependence of the rate constant can also improve the accuracy: Our ratios $k_{\text{QI}}(T)/k_{\text{QI}}(1500\text{ K})$ for both the Eckart barrier and the $\text{H} + \text{H}_2 \rightarrow \text{H}_2 + \text{H}$ reaction have somewhat smaller relative errors than the errors obtained for the absolute QI rate constants in previous studies of these systems.^{28,34} The smaller relative error in the ratio of rate constants is due to a favorable cancellation of various systematic errors, such as the systematic error of about 25% of the QI model at high temperatures (that can also be removed by an ad hoc correction of ΔH)²⁸ and small recrossing effects in the $\text{H} + \text{H}_2 \rightarrow \text{H}_2 + \text{H}$ reaction, also at high temperatures.

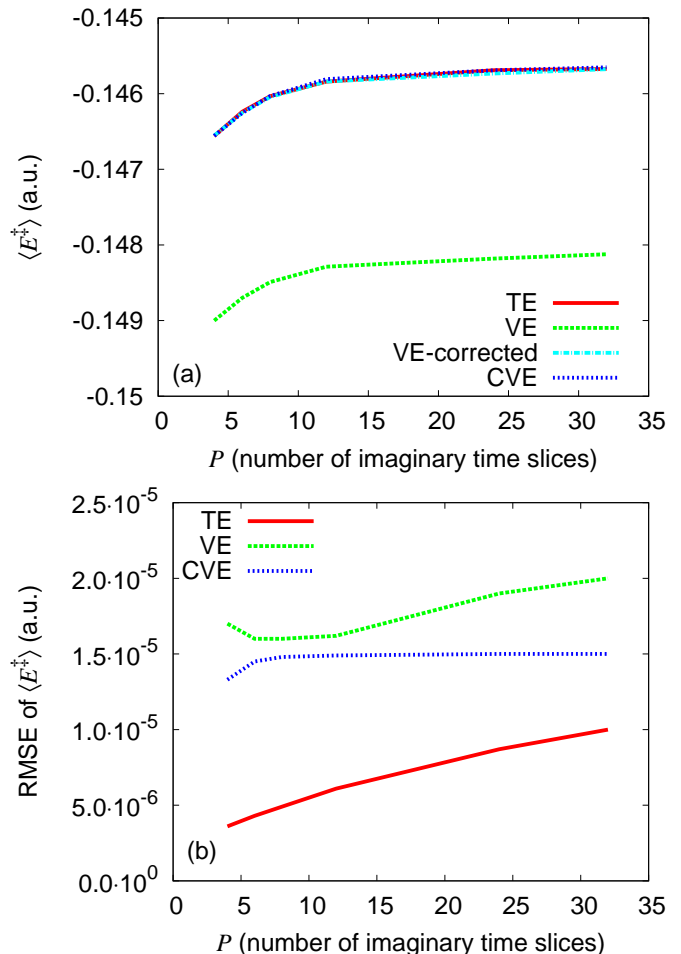


FIG. 7: Dependence of the transition state energy (a) and of the statistical RMSE of the transition state energy (b) on the number of imaginary time slices for the $\text{H} + \text{H}_2 \rightarrow \text{H}_2 + \text{H}$ reaction at $T = 515.15\text{ K}$. The constraint potential is independent of temperature and estimators (2.24)-(2.26) are used.

It is noteworthy that for both reactions, the RMSEs of transition state energies depend on the strength of the constraint. Weakening the constraint facilitates sampling of the configuration space and the error of the CVE decreases, approaching the well-known unconstrained situation where the CVE is typically the optimal estimator. However, at the same time the constraint must be strong enough to exert the constraining effect and describe the situation near the transition state properly. As a result, “ranking” of the estimators is not universal but can change with the potential used as a constraint and is in general different from the ranking for unconstrained simulations.

The dependence of the error of the VE on P is best understood in terms of the ring polymer interpretation⁷¹ of the discretized PI: The quantum thermodynamics of the original system can be interpreted as the classical thermodynamics of the ring polymer. The constrained PI simulation for the one-dimensional Eckart barrier is

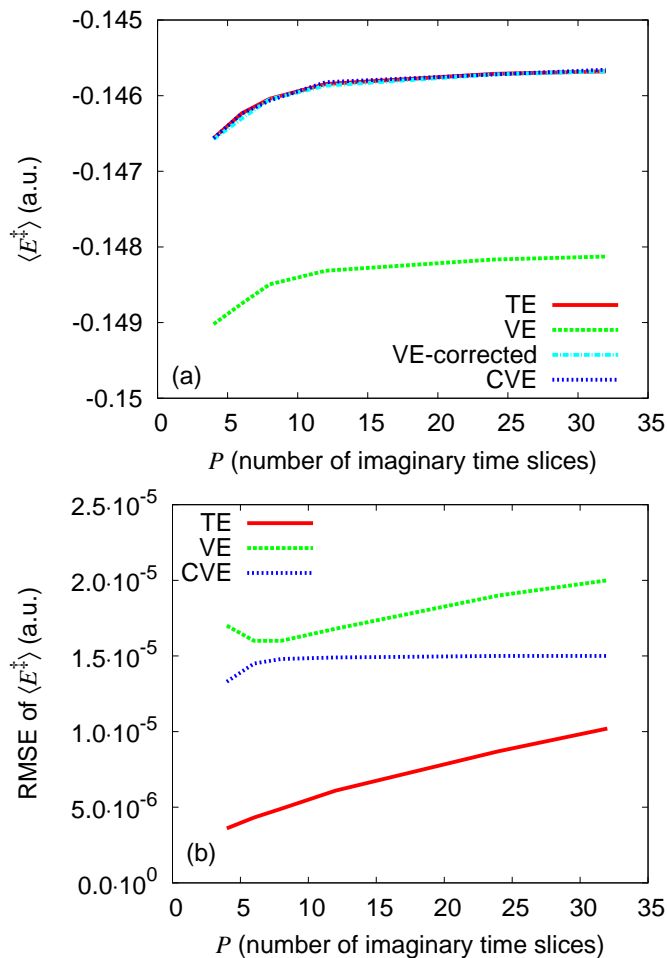


FIG. 8: Dependence of the transition state energy (a) and of the statistical RMSE of the transition state energy (b) on the number of imaginary time slices for the $\text{H} + \text{H}_2 \rightarrow \text{H}_2 + \text{H}$ reaction at $T = 515.15$ K. The constraint potential is proportional to temperature and estimators (2.24)-(2.26) are used.

completely bound, resulting in the RMSE independent of P . In the full-dimensional hydrogen exchange reaction, on the other hand, even the constrained simulation allows the system to move as a whole. This is exactly where the VE is known to have a RMSE increasing with P .

The CVE estimator is usually the optimal estimator in unconstrained systems with some translational (i.e., free-particle) degrees of freedom. In a system in which only two slices are bound (in our case, slices $P/2$ and P), the symmetry between different slices is lost and so is, to some extent, the advantage of subtracting the centroid. This explains why the RMSE of the VE can sometimes be smaller than the RMSE of the CVE for all values of P , which we observed in Figs. 3 and 4.

To sum up, while in generic systems at very low temperatures, the CVE is expected to be the optimal estimator for energy, at finite temperatures in constrained simulations, the VE or even the TE can have the smallest RMSE. The results obtained in this paper can serve as a guide for choosing the best estimator for a given system. However, since the additional cost of evaluating all three estimators is negligible in comparison to the cost of the PIMC random walk or PIMD simulation, we recommend computing all three estimators, evaluating their RMSEs, and using the one with the smallest RMSE in a given situation.

VI. ACKNOWLEDGMENTS

This research was supported by the Swiss NSF (Grant No. 200021_124936/1) and by the EPFL. Authors thank Tomáš Zimmermann for helpful discussions.

* Electronic address: jiri.vanicek@epfl.ch

- ¹ R. M. I. Elsamra, S. Vrancks, and S. A. Carl, *J. Phys. Chem. A* **109**, 10287 (2005).
- ² A. Perksy, *Chem. Phys. Lett.* **439**, 3 (2007).
- ³ M. Baasandorj, S. Griffith, S. Dusanter, and P. S. Stevens, *J. Phys. Chem. A* **113**, 10495 (2009).
- ⁴ D. C. Clary, *Science* **321**, 789 (2008).
- ⁵ W. Hu and G. C. Schatz, *J. Chem. Phys.* **125**, 132301 (2006).
- ⁶ A. Kohen, R. Cannio, S. Bartolucci, and J. P. Klinman, *Nature* **399**, 496 (1999).
- ⁷ J. Basran, M. J. Sutcliffe, and N. S. Scrutton, *Biochemistry* **38**, 3218 (1999).
- ⁸ R. A. Marcus, *J. Chem. Phys.* **125**, 194504 (2006).
- ⁹ J. Gao, D. T. Major, Y. Fan, Y. L. Lin, S. Ma, and K. Y. Wong, *Methods Mol Biol.* **443**, 37 (2008).
- ¹⁰ B. A. Ellingson and D. G. Truhlar, *J. Am. Chem. Soc.* **129**, 12765 (2007).
- ¹¹ S. Arrhenius, *Z. physik. Chem.* **4**, 226 (1889).

- ¹² H. Eyring, *J. Chem. Phys.* **3**, 107 (1935).
- ¹³ M. G. Evans and M. Polanyi, *Trans. Faraday Soc.* **31**, 875 (1935).
- ¹⁴ E. Wigner, *Trans. Faraday Soc.* **34**, 29 (1938).
- ¹⁵ E. P. Wigner, *Z. Physik. Chem.* **B19**, 203 (1932).
- ¹⁶ W. H. Miller, *Adv. Chem. Phys.* **25**, 69 (1974).
- ¹⁷ S. Chapman, B. C. Garrett, and W. H. Miller, *J. Chem. Phys.* **63**, 2710 (1975).
- ¹⁸ W. H. Miller, *J. Phys. Chem.* **105**, 2942 (2001).
- ¹⁹ W. P. Hu, Y. P. Liu, and D. G. Truhlar, *J. Chem. Soc. Faraday T.* **90**, 1715 (1994).
- ²⁰ J. W. Tromp and W. H. Miller, *J. Phys. Chem.* **90**, 3482 (1986).
- ²¹ G. A. Voth, D. Chandler, and W. H. Miller, *J. Phys. Chem.* **93**, 7009 (1989).
- ²² J. K. Hwang, Z. T. Chu, A. Yadav, and A. Warshel, *J. Phys. Chem.* **95**, 8445 (1991).
- ²³ T. N. Truong, D. Lu, G. C. Lynch, Y.-P. Liu, V. S. Melissas, J. J. P. Stewart, R. Steckler, B. C. Garrett, A. D.

- Isaacson, A. Gonzalez-Lafont, et al., *Comput. Phys. Commun.* **75**, 143 (1993).
- ²⁴ N. F. Hansen and H. C. Andersen, *J. Phys. Chem.* **100**, 1137 (1996).
- ²⁵ G. Krilov, E. Sim, and B. J. Berne, *J. Chem. Phys.* **114**, 1075 (2001).
- ²⁶ T. Wu, H.-J. Werner, and U. Manthe, *Science* **306**, 2227 (2004).
- ²⁷ R. Schubert, H. Waalkens, and S. Wiggins, *Few-Body Syst.* **45**, 2003 (2009).
- ²⁸ W. H. Miller, Y. Zhao, M. Ceotto, and S. Yang, *J. Chem. Phys.* **119**, 1329 (2003).
- ²⁹ D. Chandler, *Introduction to Modern Statistical Mechanics* (Oxford University Press, 1987).
- ³⁰ D. Frenkel and B. Smit, *Understanding Molecular Simulation* (Academic Press, 2002).
- ³¹ M. Ceotto and W. H. Miller, *J. Chem. Phys.* **120**, 6356 (2004).
- ³² S. L. Mielke, K. A. Peterson, D. W. Schwenke, B. C. Garrett, D. G. Truhlar, J. V. Michael, M.-C. Su, and J. W. Sutherland, *Phys. Rev. Lett.* **91**, 063201 (2003).
- ³³ F. J. Aoiz, L. Banares, and V. J. Herrero, *Int. Rev. Phys. Chem.* **24**, 119 (2005).
- ³⁴ T. Yamamoto and W. H. Miller, *J. Chem. Phys.* **120**, 3086 (2004).
- ³⁵ J. Vaníček, W. H. Miller, J. F. Castillo, and F. J. Aoiz, *J. Chem. Phys.* **123**, 054108 (2005).
- ³⁶ J. V. Michael, J. R. Fisher, J. M. Bowman, and Q. Sun, *Science* **249**, 269 (1990).
- ³⁷ B. K. Kendrick, *J. Phys. Chem. A* **107**, 6739 (2003).
- ³⁸ B. Lepetit and A. Kuppermann, *Chem. Phys. Lett.* **166**, 581 (1990).
- ³⁹ M. Ceotto, S. Yang, and W. H. Miller, *J. Chem. Phys.* **122**, 044109 (2005).
- ⁴⁰ M. Ceotto and W. H. Miller, private communication.
- ⁴¹ W. H. Miller, S. D. Schwartz, and J. W. Tromp, *J. Chem. Phys.* **79**, 4889 (1983).
- ⁴² Y. Zhao, T. Yamamoto, and W. H. Miller, *J. Chem. Phys.* **120**, 3100 (2004).
- ⁴³ T. Yamamoto and W. H. Miller, *J. Chem. Phys.* **122**, 044106 (2005).
- ⁴⁴ Y. Li and W. H. Miller, *Mol. Phys.* **103**, 203 (2004).
- ⁴⁵ J. Vaníček and W. H. Miller, *J. Chem. Phys.* **127**, 114309 (2007).
- ⁴⁶ W. Wang and Y. Zhao, *J. Chem. Phys.* **130**, 114708 (2009).
- ⁴⁷ T. Zimmermann and J. Vaníček, *J. Mol. Model.* (2010).
- ⁴⁸ R. Feynman and A. Hibbs, *Quantum Mechanics and Path Integrals* (McGraw-Hill, 1965).
- ⁴⁹ R. Topper, *Adv. Chem. Phys.* **105**, 117 (1999).
- ⁵⁰ B. J. Berne and D. Thirumalai, *Annu. Rev. Phys. Chem.* **37**, 401 (1986).
- ⁵¹ H. Kleinert, *Path Integrals in Quantum Mechanics, Statistics, Polymer Physics and Financial Markets* (World Scientific Publishing Co. Pte. Ltd., 2004).
- ⁵² D. M. Ceperley, *Rev. Mod. Phys.* **67**, 279 (1995).
- ⁵³ M. E. Tuckerman and G. J. Martyna, *J. Phys. Chem. B* **104**, 159 (2000).
- ⁵⁴ J. A. Barker, *J. Chem. Phys.* **70**, 2914 (1979).
- ⁵⁵ M. Herman, E. Bruskin, and B. Berne, *J. Chem. Phys.* **76**, 5150 (1982).
- ⁵⁶ M. Parrinello and A. Rahman, *J. Chem. Phys.* **80**, 860 (1984).
- ⁵⁷ K. R. Glaesemann and L. E. Fried, *J. Chem. Phys.* **116**, 5951 (2002).
- ⁵⁸ C. Predescu and J. D. Doll, *J. Chem. Phys.* **117**, 7448 (2002).
- ⁵⁹ C. Predescu, D. Sabo, J. D. Doll, and D. L. Freeman, *J. Chem. Phys.* **119**, 10475 (2003).
- ⁶⁰ C. Predescu, D. Sabo, J. D. Doll, and D. L. Freeman, *J. Chem. Phys.* **119**, 12119 (2003).
- ⁶¹ J. Vaníček and W. H. Miller, In *Proceedings of the 8th International Conference: Path Integrals from Quantum Information to Cosmology* ed. C. Burdik, O. Navratil, and S. Posta (JINR, Dubna, 2005).
- ⁶² T. Zimmermann and J. Vaníček, *J. Chem. Phys.* **131**, 024111 (2009).
- ⁶³ S. Yang, T. Yamamoto, and W. H. Miller, *J. Chem. Phys.* **124**, 084102 (2006).
- ⁶⁴ M. Sprik, M. L. Klein, and D. Chandler, *Phys. Rev. B* **31**, 4234 (1985).
- ⁶⁵ M. Kress, *Numerical Analysis* (Springer, 1998).
- ⁶⁶ H. Flyvbjerg and H. G. Petersen, *J. Chem. Phys.* **91**, 461 (1989).
- ⁶⁷ H. S. Johnston, *Gas Phase Reaction Rate Theory* (Ronald, New York, 1966).
- ⁶⁸ A. I. Boothroyd, W. J. Keogh, P. G. Martin, and M. R. Peterson, *J. Chem. Phys.* **95**, 4343 (1991).
- ⁶⁹ A. I. Boothroyd, W. J. Keogh, P. G. Martin, and M. R. Peterson, *J. Chem. Phys.* **104**, 7139 (1996).
- ⁷⁰ URL <http://www.cita.utoronto.ca/~boothroy/bkmp2.html>.
- ⁷¹ D. Chandler and P. G. Wolynes, *J. Chem. Phys.* **74**, 4078 (1981).